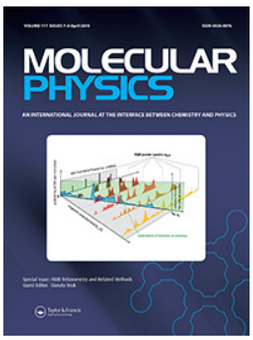

Taylor & Francis
Taylor & Francis Group

Molecular Physics

An International Journal at the Interface Between Chemistry and Physics

ISSN: 0026-8976 (Print) 1362-3028 (Online) Journal homepage: https://www.tandfonline.com/loi/tmph20

Theory of fast field-cycling NMR relaxometry of liquid systems undergoing chemical exchange

Pascal H. Fries & Elie Belorizky

To cite this article: Pascal H. Fries & Elie Belorizky (2019) Theory of fast field-cycling NMR relaxometry of liquid systems undergoing chemical exchange, Molecular Physics, 117:7-8, 849-860, DOI: 10.1080/00268976.2018.1538539

To link to this article: https://doi.org/10.1080/00268976.2018.1538539

© 2019 The Author(s). Published by Informa UK Limited, trading as Taylor & Francis Group

Published online: 15 Nov 2018.

Submit your article to this journal

Article views: 847

View related articles

View Crossmark data

Citing articles: 2 View citing articles

Full Terms & Conditions of access and use can be found at
https://www.tandfonline.com/action/journalInformation?journalCode=tmph20

MOLECULAR PHYSICS
2019, VOL. 117, NOS. 7–8, 849–860
https://doi.org/10.1080/00268976.2018.1538539

Taylor & Francis
Taylor & Francis Group

NMR RELAXOMETRY AND RELATED METHODS

OPEN ACCESS Check for updates

Theory of fast field-cycling NMR relaxometry of liquid systems undergoing chemical exchange

Pascal H. Fries[a] and Elie Belorizky[b,c]

[a]INAC/MEM CEA, Univ. Grenoble Alpes, Grenoble, France; [b]CEA-LETI, Grenoble, France; [c]Univ. Grenoble Alpes, Grenoble, France

ABSTRACT

The time evolution of the nuclear magnetisation of chemically exchanging systems in liquids is calculated for the pre-polarised fast field-cycling sequence of nuclear magnetic resonance (NMR) relaxometry. The obtained parameter expressions of the magnetisation allow one to derive the longitudinal relaxation rates and the residence times of the exchanging sites from the experiment. In the particular cases of slow and fast exchange, approximations leading to simple analytic expressions are derived. The theory takes account of the delay time necessary to ensure that the field for acquiring the signal is stable enough after its rapid jump from its relaxation value. The domains of mono-exponential or bi-exponential relaxation of the magnetisation are displayed in a concise way through 3D and 2D logarithmic plots of the population ratio of the exchanging sites and of their intrinsic relaxation times. The influence of the acquisition delay on the fitted values of the populations, residence times, and intrinsic relaxation times of the sites is emphasised in the case of the bi-exponential water proton relaxation observed in a tumour tissue.

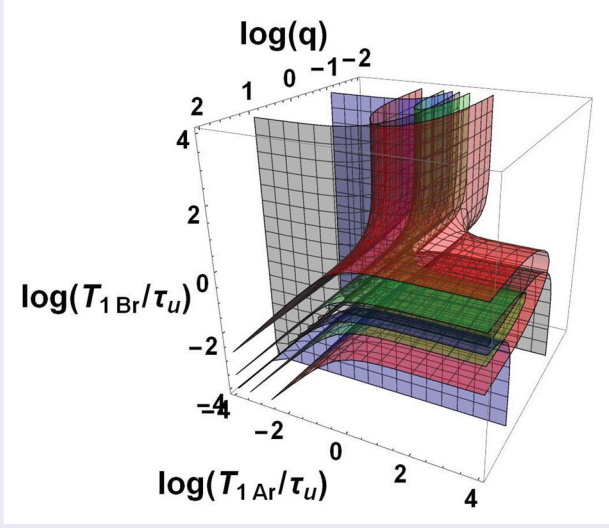

ARTICLE HISTORY
Received 30 June 2018
Accepted 11 October 2018

KEYWORDS
Magnetic resonance imaging; NMR relaxometry; fast field-cycling; chemical exchange

1. Introduction

Fast field-cycling (FFC) techniques [1,2] in both nuclear magnetic resonance (NMR) and magnetic resonance imaging (MRI) give unique information about the quantum dynamics of spins and spatial motions of molecules in liquids [3–9], in particular of water molecules in the biomedical context [2–5,8–14]. These experiments provide raw NMR relaxation data, that is the time evolution of the longitudinal magnetisation of the water protons across several orders of magnitude of the external magnetic field B_0. This time evolution probes the various sites, environments or compartments of the water molecules such as the coordination sites of metal ions and adsorption sites on macromolecules, the intra- or extracellular space in biological tissues, the vascular space in living organisms, and the bulk aqueous environment [3–5,8–17]. In the context of MRI contrast agents, and more generally of paramagnetic metal complexes in solu-

CONTACT Pascal H. Fries pascal-h.fries@cea.fr INAC/MEM CEA, Univ. Grenoble Alpes, F-38054 Grenoble, France

© 2019 The Author(s). Published by Informa UK Limited, trading as Taylor & Francis Group
This is an Open Access article distributed under the terms of the Creative Commons Attribution License (http://creativecommons.org/licenses/by/4.0/), which permits unrestricted use, distribution, and reproduction in any medium, provided the original work is properly cited.

tion, numerous FFC-NMR experiments were performed to study the Brownian modulation of anisotropic electronic spin Hamiltonians, such as those related to the zero-field splitting (ZFS), the hyperfine coupling, and the g factor [3–6]. Usually, water molecules do not remain confined in a given site, but exchange between adjacent sites. The lifetimes or residence times τ_{site} of a water molecule in its various accessible sites ($site = A, B$) are fundamental parameters which characterise these sites and their interactions. The lifetimes τ_{site} and the intrinsic NMR relaxation rates R_{1site} of the sites can be determined from NMR relaxation data. In a protein aqueous solution, where water exchanges between protein binding sites and free bulk water sites, the rotational correlation time τ_R [8,10] of the protein macromolecules can be derived together with the parameters τ_{site} and R_{1site} from nuclear magnetic relaxation dispersions (NMRD), provided that τ_R is shorter than the lifetime of a water molecule bound to a tumbling protein. The time τ_R is a key determinant of the aggregation of the proteins, hence of the feasibility and quality of their NMR spectroscopy. The lifetimes τ_{site} can also allow one to distinguish between healthy and diseased tissues. For instance, intracellular water lifetime can be used as a biomarker of tumours and of their aggressiveness [14,16]. More generally, profiles of NMR relaxation rates as a function of the field over several decades are expected to yield completely new biomarkers of diseases, especially in the low and ultra-low field domains [2,11–14,18].

In liquid systems, the influence of chemical exchange between two sites on the evolution of the magnetisation of the nuclei of the exchanging species is a standard problem at a fixed external magnetic field [19–21]. However, in an FFC-NMR or MRI experiment, the external field takes very different values during the evolution of the nuclear magnetisation. Then, the evolution of the magnetisations of the two sites is no longer given by the usual solution of the Bloch–McConnell equations. The aim of this paper is to provide a theoretical framework suitable to extract the lifetimes and intrinsic relaxation rates R_1 of the sites at any value of the relaxation field from the ultra-low regime below earth field up to several T.

The article is organised as follows. Section 2 provides the solution of the Bloch–McConnell equations in a form suitable to express the time evolution of the nuclear magnetisation during any FFC sequence. The general expression of the signal, which results from this time evolution and can be observed at the end of the sequence, is derived in Section 3 for the important pre-polarised (PP) sequence. The limiting cases of slow and fast chemical exchange lead to simple analytical expressions of the signal which are detailed in Section 4. Finally, the relaxometric exploration of systems undergoing chemical exchange is discussed in terms of the site populations and intrinsic relaxation rates in Section 5.

2. Convenient expression of the solution of the Bloch–McConnell equations

In a fixed external field $\mathbf{B}_0$ along the z-axis, consider nuclear spins I of the same isotope. Through chemical exchange, these spins alternately occupy two different relaxation sites A and B corresponding to different molecular environments. The spins of sites A, B have population fractions p_A, p_B with $p_A + p_B = 1$. Their residence times are τ_A, τ_B which verify the detailed balance principle $\tau_B/\tau_A = p_B/p_A$. Their magnetic susceptibilities are $\chi_A = p_A\chi$, $\chi_B = p_B\chi$ where $\chi = \chi_A + \chi_B$ is the total magnetic susceptibility of the spins of the two sites. Their time-dependent magnetisations along the z axis are $M_{Az} = p_A M_z$, $M_{Bz} = p_B M_z$, M_z being the total magnetisation. In the field value B_v, they have equilibrium magnetisations $M_{Av}^{eq} = \chi_A B_v$, $M_{Bv}^{eq} = \chi_B B_v$, intrinsic relaxation times T_{1Av}, T_{1Bv}, and intrinsic relaxation rates $R_{1Av} = 1/T_{1Av}$, $R_{1Bv} = 1/T_{1Bv}$. For any property m with values m_A, m_B at sites A, B, the property column is defined as $\tilde{m} = \begin{pmatrix} m_A \\ m_B \end{pmatrix}$. The Bloch–McConnell equations read [19–21]

$$\begin{aligned} \frac{\mathrm{d}M_{Az}}{\mathrm{d}t} &= -\frac{1}{T_{1Av}}(M_{Az} - M_{Av}^{eq}) - \frac{M_{Az}}{\tau_A} + \frac{M_{Bz}}{\tau_B}, \\ \frac{\mathrm{d}M_{Bz}}{\mathrm{d}t} &= -\frac{1}{T_{1Bv}}(M_{Bz} - M_{Bv}^{eq}) - \frac{M_{Bz}}{\tau_B} + \frac{M_{Az}}{\tau_A}. \end{aligned} \tag{1}$$

Introduce the α relaxation parameters

$$\alpha_{Av} = \frac{1}{T_{1Av}} + \frac{1}{\tau_A}, \quad \alpha_{Bv} = \frac{1}{T_{1Bv}} + \frac{1}{\tau_B} \tag{2}$$

and the relaxation matrix

$$R_v = \begin{pmatrix} \alpha_{Av} & -\tau_B^{-1} \\ -\tau_A^{-1} & \alpha_{Bv} \end{pmatrix} \tag{3}$$

Using the detailed balance principle, the Bloch–McConnell equations can be rewritten in matrix form in terms of the magnetisation column $\tilde{M}_z = \begin{pmatrix} M_{Az} \\ M_{Bz} \end{pmatrix}$ and its equilibrium value $\tilde{M}_v^{eq} = \begin{pmatrix} M_{Av}^{eq} \\ M_{Bv}^{eq} \end{pmatrix}$ as

$$\frac{\mathrm{d}}{\mathrm{d}t}\tilde{M}_z = -R_v(\tilde{M}_z - \tilde{M}_v^{eq}). \tag{4}$$

Introduce the residual magnetisation column $\tilde{m}_{vz} = \tilde{M}_z - \tilde{M}_v^{eq}$. Equation (4) is equivalent to

$$\frac{\mathrm{d}}{\mathrm{d}t}\tilde{m}_{vz} = -R_v\tilde{m}_{vz}. \tag{5}$$

The eigenvalues of the relaxation matrix R_v are the fast and slow effective relaxation rates R_v^+ and R_v^-, respectively defined as

$$R_v^{\pm} = \frac{1}{2}\left[(\alpha_{Av} + \alpha_{Bv}) \pm \sqrt{(\alpha_{Av} - \alpha_{Bv})^2 + 4\tau_A^{-1}\tau_B^{-1}}\right]. \tag{6}$$

Introducing the coefficients

$$\mu_v^{\pm} = (\alpha_{Av} - R_v^{\pm})\tau_B, \tag{7}$$

their difference

$$D_v = \mu_v^- - \mu_v^+, \tag{8}$$

and the enhancement factors

$$\kappa_v^{\pm} = 1 + \mu_v^{\pm}, \tag{9}$$

the matrix P_v of the eigenvectors associated to R_v^+, R_v^- and its inverse P_v^{-1} are

$$P_v = \begin{pmatrix} 1 & 1 \\ \mu_v^+ & \mu_v^- \end{pmatrix} \quad \text{and} \quad P_v^{-1} = \frac{1}{D_v}\begin{pmatrix} \mu_v^- & -1 \\ -\mu_v^+ & 1 \end{pmatrix}, \tag{10}$$

where D_v is the determinant of P_v. The matrix R_v can be rewritten as

$$R_v = P_v \begin{pmatrix} R_v^+ & 0 \\ 0 & R_v^- \end{pmatrix} P_v^{-1}. \tag{11}$$

At the initial time t_i, assume that the magnetisation column $\tilde{m}_{zv}$ is $\tilde{m}_{zv}(t_i) = \begin{pmatrix} m_{Azv}(t_i) \\ m_{Bzv}(t_i) \end{pmatrix}$. The general solution of Equation (5) at time $t \geq t_i$ is

$$\tilde{m}_{zv}(t) = \mathrm{e}^{-R_v(t-t_i)}\tilde{m}_{zv}(t_i), \tag{12}$$

where the exponential relaxation matrix $\mathrm{e}^{-R_v u}$ can be expressed as

$$\mathrm{e}^{-R_v u} = P_v \begin{pmatrix} \mathrm{e}^{-R_v^+ u} & 0 \\ 0 & \mathrm{e}^{-R_v^- u} \end{pmatrix} P_v^{-1}. \tag{13}$$

Replacing P_v and P_v^{-1} by their expressions of Equation (10), Equation (13) can be rewritten as

$$\mathrm{e}^{-R_v u} = \mathrm{e}^{-R_v^+ u}\Lambda_v^+ + \mathrm{e}^{-R_v^- u}\Lambda_v^- \tag{14}$$

with

$$\Lambda_v^+ = \frac{1}{D_v}\begin{pmatrix} \mu_v^- & -1 \\ \mu_v^+\mu_v^- & -\mu_v^+ \end{pmatrix},$$
$$\Lambda_v^- = \frac{1}{D_v}\begin{pmatrix} -\mu_v^+ & 1 \\ -\mu_v^-\mu_v^+ & \mu_v^- \end{pmatrix}. \tag{15}$$

Note that the matrix-column product of $\Lambda_v^{\pm}$ by a column $\tilde{m} = \begin{pmatrix} m_A \\ m_B \end{pmatrix}$ is given by

$$\Lambda_v^{\pm}\tilde{m} = c_v^{\pm}[\tilde{m}]\begin{pmatrix} 1 \\ \mu_v^{\pm} \end{pmatrix}, \tag{16}$$

where the auxiliary linear functions $c_v^{\pm}$ take scalar values and are defined as

$$c_v^{\pm}[\tilde{m}] = c_v^{\pm}\begin{pmatrix} m_A \\ m_B \end{pmatrix} = \frac{1}{D_v}(\pm\mu_v^{\mp}m_A \mp m_B). \tag{17}$$

Then, the solution of Equations (1) or (4) is the image of the initial magnetisation column $\tilde{M}_z(t_i)$ by the evolution operator $E_v(t - t_i)$ defined as the affine transformation

$$\begin{aligned}\tilde{M}_z(t) &= E_v(t - t_i)\tilde{M}_z(t_i) \\ &= \tilde{\chi}B_v + \mathrm{e}^{-R_v(t-t_i)}[\tilde{M}_z(t_i) - \tilde{\chi}B_v],\end{aligned} \tag{18}$$

with $\tilde{\chi} = \begin{pmatrix} \chi_A \\ \chi_B \end{pmatrix}$ and $\mathrm{e}^{-R_v(t-t_i)}$ given by Equations (14)–(17).

3. Time evolution of the nuclear magnetisation during the pre-polarised sequence and observed signal

The PP sequence [1] is a typical FFC sequence of successive different field values which is sketched in Figure 1. The PP sequence allows one to explore the evolution of the nuclear magnetisation at low field and to derive the intrinsic relaxation rates of the studied nuclei and their lifetimes in their different sites.

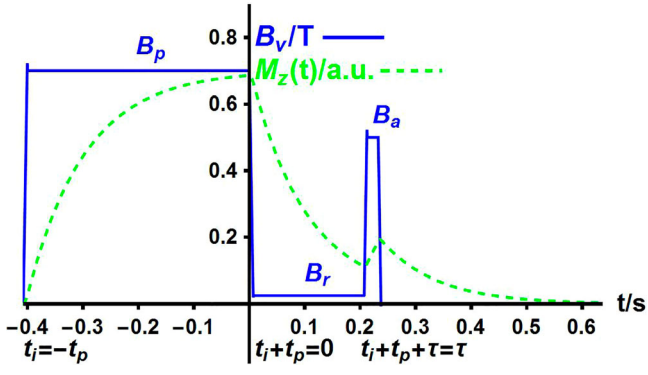

Figure 1. Basic cycle of the magnetic field $B_v(t)$ (continuous line) in a pre-polarised (PP) sequence. The field B_v successively takes the polarisation value B_p for a polarisation time t_p, the relaxation value B_r for an evolution time τ, the signal acquisition value B_a for an acquisition time t_a, and the zero value for a repetition delay taken to be equal to t_p. The nuclear magnetisation $M_z(t)$ (dotted line) in arbitrary units tends to its instantaneous equilibrium value $\chi B_v(t)$ so that it evolves as the field $B_v(t)$ with some delay. The time origin is conveniently taken to be at the start of the evolution period τ.

Turn to the description of the PP sequence and to the related theoretical expression of the evolution of the magnetisation column during this sequence. The applied magnetic field B_v successively takes the polarisation value B_p, typically between 0.2 and 1 T, for a fixed polarisation duration t_p, the relaxation value B_r during the variable evolution time τ, and the acquisition value B_a during the fixed acquisition time t_a taken to be somewhat longer than the delay s required to ensure field stability. Since relaxation at field B_r is investigated by varying τ, the time origin is taken to be the start of the evolution period. The magnetisation column $\tilde{M}_z$ at time $\tau + s$ is calculated by successive applications of the operators $E_p(t_p)$, $E_r(\tau)$, and $E_a(s)$. It reads

$$\tilde{M}_z(\tau+s) \equiv \begin{pmatrix} M_{Az}(\tau+s) \\ M_{Bz}(\tau+s) \end{pmatrix} = E_a(s)E_r(\tau)E_p(t_p)\tilde{M}_z(t_i=-t_p). \quad (19)$$

The observed signal is the free induction decay (FID) obtained by applying a 90° pulse at the stabilised acquisition field B_a after the acquisition delay s. It is proportional to the total longitudinal magnetisation $M_z(\tau+s) = M_{Az}(\tau+s) + M_{Bz}(\tau+s)$. Finally, after recording the FID, the applied magnetic field B_v is switched off to zero during a fixed repetition delay t_d of the order of the polarisation duration t_p before repetition (cycling) of the sequence. The repetition delay is chosen so that the magnetisations of both sites are zero before the start of a new cycle. In Figure 1, note that the field B_v displays sudden jumps at times $t_i = -t_p, t_i + t_p = 0, t_i + t_p + \tau = \tau$, and after the acquisition of the FID, though field ramps occur in practice. The magnetisations $M_{Az}(t)$, $M_{Bz}(t)$ remain constant across these ideal field jumps.

Assume that the polarisation period t_p is longer than $4\max(T_{1Ap}, T_{1Bp})$, where T_{1Ap}, T_{1Bp} are the intrinsic relaxation times in the polarisation field B_p. Then, the magnetisation column $\tilde{M}_z$ reaches its equilibrium value $\tilde{M}_p^{eq} = \tilde{\chi}B_p$ at the end of the polarisation period so that $\tilde{M}_z(0) = E_p(t_p)\tilde{M}_z(t_i=-t_p) = \tilde{M}_p^{eq}$. Replacing $E_a(s)$ and $E_r(\tau)$ by their affine expressions in Equation (18) and setting

$$\tilde{m}_{zr}(0) = \begin{pmatrix} m_{Azr}(0) \\ m_{Bzr}(0) \end{pmatrix} \equiv \tilde{m}_{zr}^0 = \begin{pmatrix} m_{Azr}^0 \\ m_{Bzr}^0 \end{pmatrix} = \tilde{M}_z(0) - \tilde{\chi}B_r = \begin{pmatrix} M_{Az}(0) - \chi_A B_r \\ M_{Bz}(0) - \chi_B B_r \end{pmatrix}, \quad (20)$$

Equation (19) simplifies to

$$\begin{aligned}\tilde{M}_z(\tau+s) &= E_a(s)E_r(\tau)\tilde{M}_z(0) \\ &= E_a(s)\{\tilde{\chi}B_r + \mathrm{e}^{-R_r\tau}[\tilde{M}_z(0) - \tilde{\chi}B_r]\} \\ &= \tilde{\chi}B_a + \mathrm{e}^{-R_a s}\tilde{\chi}(B_r - B_a) \\ &\quad + \mathrm{e}^{-R_a s}\mathrm{e}^{-R_r\tau}\tilde{m}_{rz}(0) \end{aligned} \quad (21)$$

Replacing $\mathrm{e}^{-R_a s}$ and $\mathrm{e}^{-R_r\tau}$ by their expressions in Equation (14) with $\Lambda_v^{\pm}$ $(v = r, s)$ given by Equations (16) and (17), $\tilde{M}_z(\tau+s)$ can be rewritten as

$$\tilde{M}_z(\tau+s) \equiv \begin{pmatrix} M_{Az}(\tau+s) \\ M_{Bz}(\tau+s) \end{pmatrix} = \tilde{C}^0(s) + e^{-R_r^+\tau}\tilde{C}^+(s) + e^{-R_r^-\tau}\tilde{C}^-(s) \quad (22)$$

where the columns $\tilde{C}^0(s)$, $\tilde{C}^{\pm}(s)$ are defined as

$$\begin{aligned}\tilde{C}^0(s) &= \tilde{\chi}B_a + \left[\mathrm{e}^{-R_a^+ s}\frac{1}{D_a}(\mu_a^-\chi_A - \chi_B)\begin{pmatrix}1\\ \mu_a^+\end{pmatrix} + \mathrm{e}^{-R_a^- s}\frac{1}{D_a}(-\mu_a^+\chi_A + \chi_B)\begin{pmatrix}1\\ \mu_a^-\end{pmatrix}\right](B_r - B_a) \\ \tilde{C}^{\pm}(s) &= c_r^{\pm}[\tilde{m}_{zr}(0)]\left[\mathrm{e}^{-R_a^+ s}\frac{1}{D_a}(\mu_a^- - \mu_r^{\pm})\begin{pmatrix}1\\ \mu_a^+\end{pmatrix} + \mathrm{e}^{-R_a^- s}\frac{1}{D_a}(-\mu_a^+ + \mu_r^{\pm})\begin{pmatrix}1\\ \mu_a^-\end{pmatrix}\right] \end{aligned} \quad (23)$$

with

$$\begin{aligned} c_r^+[\tilde{m}_{zr}(0)] &= \frac{1}{D_r}(\mu_r^- m_{Azr}(0) - m_{Bzr}(0)), \\ c_r^-[\tilde{m}_{zr}(0)] &= \frac{1}{D_r}(-\mu_r^+ m_{Azr}(0) + m_{Bzr}(0)), \end{aligned} \quad (24)$$

and $m_{Azr}(0) = M_{Az}(0) - \chi_A B_r$, $m_{Bzr}(0) = M_{Bz}(0) - \chi_B B_r$.

The NMR signal is proportional to

$$\begin{aligned} M_z(\tau+s) &= M_{Az}(\tau+s) + M_{Bz}(\tau+s) \\ &= w^0(s) + w^+(s)\mathrm{e}^{-R_r^+\tau} + w^-(s)\mathrm{e}^{-R_r^-\tau}, \end{aligned} \quad (25)$$

where the coefficients $w^0(s)$, $w^{\pm}(s)$ are defined as

$$\begin{aligned} w^0(s) &= \chi B_a + \left[\mathrm{e}^{-R_a^+ s}\frac{\kappa_a^+}{D_a}(\mu_a^-\chi_A - \chi_B) + \mathrm{e}^{-R_a^- s}\frac{\kappa_a^-}{D_a}(-\mu_a^+\chi_A + \chi_B)\right](B_r - B_a) \\ w^{\pm}(s) &= c_r^{\pm}[\tilde{m}_{zr}(0)]\left[\mathrm{e}^{-R_a^+ s}\frac{\kappa_a^+}{D_a}(\mu_a^- - \mu_r^{\pm}) + \mathrm{e}^{-R_a^- s}\frac{\kappa_a^-}{D_a}(-\mu_a^+ + \mu_r^{\pm})\right], \end{aligned} \quad (26)$$

with $\kappa_a^{\pm}$ defined by Equation (9) and $c_r^{\pm}[\tilde{m}_{zr}(0)]$ given by Equation (24).

Turn to the limiting case $s = 0$. According to Equations (22) and (23), the column magnetisation becomes

$$\tilde{M}_z(\tau) \equiv \begin{pmatrix} M_{zA}(\tau) \\ M_{zB}(\tau) \end{pmatrix} = \tilde{C}^0(0) + e^{-R_r^+\tau}\tilde{C}^+(0) + e^{-R_r^-\tau}\tilde{C}^-(0), \quad (27)$$

with the columns

$$\tilde{C}^0(0) = \tilde{\chi}B_r, \quad \tilde{C}^{\pm}(0) = c_r^{\pm}[\tilde{m}_{zr}(0)]\begin{pmatrix} 1 \\ \mu_r^{\pm} \end{pmatrix}. \quad (28)$$

Then, the NMR signal is proportional to

$$M_z(\tau) = w^0(0) + w^+(0)e^{-R_r^+\tau} + w^-(0)e^{-R_r^-\tau}, \quad (29)$$

with the coefficients

$$\begin{aligned} w^0(0) &= \chi B_r, \\ w^+(0) &= \frac{\kappa_r^+}{D_r}[\mu_r^- m_{Azr}(0) - m_{Bzr}(0)], \\ w^-(0) &= \frac{\kappa_r^-}{D_r}[-\mu_r^+ m_{Azr}(0) + m_{Bzr}(0)]. \end{aligned} \quad (30)$$

The expressions of the coefficients $w^{\pm}(0)$ can be simplified. Introducing the discriminant $\overline{\Delta}_r = \sqrt{(R_{1Br} - R_{1Ar} + \tau_B^{-1} - \tau_A^{-1})^2 + 4\tau_A^{-1}\tau_B^{-1}}$, the coefficients $w^{\pm}(0)$ in Equation (30) can be rewritten as rational fractions in $\overline{\Delta}_r$. Replacing $\overline{\Delta}_r^2$ by its expression in terms of R_{1Ar}, R_{1Br}, τ_A^{-1}, τ_B^{-1} and using the equality $(p_A\tau_B)^{-1} = (p_B\tau_A)^{-1} = \tau_A^{-1} + \tau_B^{-1}$, $w^{\pm}(0)$ simplify to

$$w^{\pm}(0) = (M_z(0) - \chi B_r)\frac{1}{2} \times \left[1 \mp \frac{(1-2p_B)(R_{1Br} - R_{1Ar}) + \tau_A^{-1} + \tau_B^{-1}}{\overline{\Delta}_r}\right], \quad (31)$$

with $\tau_A^{-1} = \tau_B^{-1}p_B/(1-p_B)$. Following Ruggiero *et al.* [14], consider the evolution of the magnetisation of the hydrogen nuclei of water exchanging between intra- (*in*) and extra- (*ex*) cellular compartments for the saturation recovery sequence. Setting $in = A$, $ex = B$, $v_{in} = p_A$, $v_{ex} = p_B$, according to Equations (1) and (4) of the Supporting Information of Ref. [14], the coefficients of the decreasing exponentials $e^{-R_r^+\tau}$ and $e^{-R_r^-\tau}$ with the shorter (S) and longer (L) apparent relaxation times are

$$a_S = \frac{1}{2}\left[1 - \frac{(1-2p_B)(R_{1Br} - R_{1Ar}) + \tau_A^{-1} + \tau_B^{-1}}{\overline{\Delta}_r}\right], \quad (32)$$

and $a_L = 1 - a_S$, respectively. From Equation (31), $w^+(0) = (M_z(0) - \chi B_r)a_S$ and $w^-(0) = (M_z(0) - \chi B_r) \times a_L$ are respectively proportional to a_S and a_L with the same proportionality factor $M_z(0) - \chi B_r$. Thus, the changes of $M_z(\tau)$ with time of the PP sequence and saturation recovery sequence are just proportional at any evolution time τ. For immediate acquisition $s = 0$, the difference between the two sequences is the dynamic range of $M_z(\tau)$ which decreases from $M_z(0)$ to χB_r for the PP sequence and increases from 0 to χB_r for the saturation recovery or non-polarised (NP) [1] sequence. Since the magnetisation $M_z(\tau)$ is proportional to an NMR experimental signal, which is defined up to an arbitrary multiplicative factor, $M_z(0)$ and χB_r should be considered as additional independent fit parameters when fitting the model of $M_z(\tau)$ of Equations (29) and (30) to experimental data, unless there is a relationship between χB_r and $M_z(0)$ due to the experimental conditions.

4. Particular cases

Following McLaughlin and Leigh [20], slow and fast exchange situations can be defined by comparing the effective exchange rate $1/\tau_{AB}$, the so-called 'shutter-speed' [16], and the relaxation rate difference Δ_v defined as

$$\frac{1}{\tau_{AB}} = \frac{1}{\tau_A} + \frac{1}{\tau_B} \quad \text{and} \quad \Delta_v = \frac{1}{T_{1Av}} - \frac{1}{T_{1Bv}}. \quad (33)$$

The slow and fast exchange situations are defined by the inequalities $1/\tau_{AB} << |\Delta_v|$ and $|\Delta_v| << 1/\tau_{AB}$, respectively. They depend on the field value B_v because the intrinsic relaxation rates $1/T_{1Av}$, $1/T_{1Bv}$ vary with the field.

4.1. Immediate acquisition $s = 0$

4.1.1. Slow exchange limit in the relaxation field B_r: $1/\tau_{AB} << |\Delta_r|$

For $\Delta_r > 0$, the fast and slow effective relaxation rates are

$$R_r^+ = \alpha_{Ar} = \frac{1}{T_{1Ar}} + \frac{1}{\tau_A}, \quad R_r^- = \alpha_{Br} = \frac{1}{T_{1Br}} + \frac{1}{\tau_B}. \quad (34)$$

According to Equations (7) and (34), we have $\mu_r^+ \cong 0$, $\mu_r^- \cong \Delta_r\tau_B + \tau_B/\tau_A - 1$. The slow exchange condition leads to $|\tau_B/\tau_A - 1| << |\Delta_r|\tau_B$ so that $\mu_r^- \cong \Delta_r\tau_B$ and $D_r = \mu_r^- - \mu_r^+ \cong \Delta_r\tau_B$. Since $\Delta_r = |\Delta_r|$, according to Equation (24), we have

$$\begin{aligned} c_r^+[\tilde{m}_{zr}(0)] &= m_{Azr}(0) - \frac{m_{Bzr}(0)}{|\Delta_r|\tau_B}, \\ c_r^-[\tilde{m}_{zr}(0)] &= \frac{m_{Bzr}(0)}{|\Delta_r|\tau_B}. \end{aligned} \quad (35)$$

Consequently, from Equations (27), (28), and (34), the magnetisations of sites A and B are

$$M_{Az}(\tau) = \chi_A B_r + \left[m_{Azr}(0) - \frac{m_{Bzr}(0)}{|\Delta_r|\tau_B}\right] e^{-\alpha_{Ar}\tau} + \frac{m_{Bzr}(0)}{|\Delta_r|\tau_B} e^{-\alpha_{Br}\tau}$$
$$M_{Bz}(\tau) = \chi_B B_r + m_{Bzr}(0) e^{-\alpha_{Br}\tau}. \quad (36)$$

Dropping all the terms with the factors $1/(|\Delta_r|\tau_B)$, these magnetisations reduce to

$$M_{Az}(\tau) = \chi_A B_r + m_{Azr}(0) e^{-\alpha_{Ar}\tau},$$
$$M_{Bz}(\tau) = \chi_B B_r + m_{Bzr}(0) e^{-\alpha_{Br}\tau} \quad (37)$$

Since $1 << |\Delta_r|\tau_B$, the total magnetisation derived from Equation (36) is

$$M_z(\tau) = M_{Az}(\tau) + M_{Bz}(\tau) = \chi B_r + \left[m_{Azr}(0) - \frac{m_{Bzr}(0)}{|\Delta_r|\tau_B}\right] e^{-\alpha_{Ar}\tau} + m_{Bzr}(0) e^{-\alpha_{Br}\tau}. \quad (38)$$

Except if $|m_{Azr}(0)| << |m_{Bzr}(0)|$, for instance, when $p_A << p_B$, $M_z(\tau)$ reduces to the symmetric expression

$$M_z(\tau) = \chi B_r + m_{Azr}(0) e^{-\alpha_{Ar}\tau} + m_{Bzr}(0) e^{-\alpha_{Br}\tau}. \quad (39)$$

When $\Delta_r < 0$, the values of $c_r^{\pm}[\tilde{m}_{rz}(0)]$, $M_{Az}(\tau)$, $M_{Bz}(\tau)$, and $M_z(\tau)$ are obtained by permutation of the roles of A and B. Note that under the additional conditions $1/\tau_A << 1/T_{1Ar}$ and $1/\tau_B << 1/T_{1Br}$, the total magnetisation evolves as the sum of the magnetisations of sites without exchange.

4.1.2. Fast exchange limit in the relaxation field B_r: $|\Delta_r| << 1/\tau_{AB}$

The fast exchange condition leads to the inequality $\Delta_r\tau_B << 1/p_A$. Setting

$$\frac{1}{T_{1r}} = \frac{1}{2}\left(\frac{1}{T_{1Ar}} + \frac{1}{T_{1Br}}\right), \quad (40)$$

the effective relaxation rates are

$$R_r^+ = \frac{1}{\tau_A} + \frac{1}{\tau_B} + \frac{1}{T_{1r}} + \frac{\Delta_r}{2}(p_B - p_A),$$
$$R_r^- = \frac{p_A}{T_{1Ar}} + \frac{p_B}{T_{1Br}}. \quad (41)$$

Then, we have $\alpha_A - R_r^- = \Delta_r p_B + 1/\tau_A$, $\mu_r^- = \Delta_r p_B\tau_B + p_B/p_A \cong p_B/p_A$, $\alpha_A - R_r^+ = \Delta_r p_A - 1/\tau_B$, $\mu_r^+ = \Delta_r p_A\tau_B - 1 \cong -1$, and $D_r \cong p_B/p_A + 1 = 1/p_A$. From Equation (28), we get

$$\tilde{C}^0(0) = \tilde{\chi} B_r,$$
$$\tilde{C}^+(0) = [p_B m_{Azr}(0) - p_A m_{Bzr}(0)]\begin{pmatrix}1\\-1\end{pmatrix},$$
$$\tilde{C}^-(0) = [m_{Azr}(0) + m_{Bzr}(0)]\begin{pmatrix}p_A\\p_B\end{pmatrix}, \quad (42)$$

so that the site magnetisations are

$$M_{Az}(\tau) = \chi_A B_r + [p_B m_{Azr}(0) - p_A m_{Bzr}(0)] e^{-R_r^+\tau} + [m_{Azr}(0) + m_{Bzr}(0)] p_A e^{-R_r^-\tau},$$
$$M_{Bz}(\tau) = \chi_B B_r - [p_B m_{Azr}(0) - p_A m_{Bzr}(0)] e^{-R_r^+\tau} + [m_{Azr}(0) + m_{Bzr}(0)] p_B e^{-R_r^-\tau}, \quad (43)$$

and the total magnetisation is

$$M_z(\tau) = \chi B_r + [m_{Azr}(0) + m_{Bzr}(0)] e^{-R_r^-\tau}. \quad (44)$$

The total magnetisation decays with the slow effective relaxation rate R_r^- given by Equation (41).

4.1.3. Site of scarce nuclei with high intrinsic relaxation rate

Assume that the population of site B is scarce, i.e. $p_B << 1$ and $p_A \cong 1$, with a high relaxation rate $1/T_{1Br} >> 1/T_{1Ar}$. For instance, the situation occurs in liquid solutions when A corresponds to the solvent molecules in the bulk and B to solvent molecules bound to paramagnetic species or slowly rotating macromolecules. Then, as $1/\tau_A << 1/\tau_B$, we have $\alpha_A << \alpha_B$. Then, the effective relaxation rates are

$$R_r^+ \cong \alpha_{Br}, \quad R_r^- \cong \frac{1}{T_{1Ar}} + \frac{p_B}{p_A}\frac{1}{T_{1Br} + \tau_B}. \quad (45)$$

The parameters defining the change-of-basis matrices P_r and P_r^{-1} from Equation (10) with $v = r$ are $\mu_r^- \cong \frac{p_B}{p_A}\frac{T_{1Br}}{T_{1Br}+\tau_B} << 1$, $\mu_r^+ \cong -1 - \frac{\tau_B}{T_{1Br}}$, $D_r = -\mu_r^+ \cong 1 + \frac{\tau_B}{T_{1Br}}$. By neglecting terms in $p_B/p_A = \tau_B/\tau_A$ and $m_{Br}(0)/m_{Ar}(0)$, from Equations (27) and (28), the site magnetisations can be approximated as

$$M_{Az}(\tau) = \chi_A B_r + m_{Azr}(0) e^{-R_r^-\tau},$$
$$M_{Bz}(\tau) = 0, \quad (46)$$

so that the total magnetisation is

$$M_z(\tau) \cong M_{Az}(\tau) \cong \chi B_r + m_{zr}(0) e^{-R_r^-\tau}, \quad (47)$$

The $M_z(\tau)$ evolution of Equation (47) with R_r^- given by Equation (45) overlaps the time decays obtained above

in the slow and fast exchange limits. Indeed, in the slow exchange case $T_{1Br} << \tau_B$, R_r^- in Equation (45) reduces to $R_r^- \cong 1/T_{1Ar} + (p_B/p_A)/\tau_B = 1/T_{1Ar} + 1/\tau_A = \alpha_{Ar}$, so that $M_z(\tau)$ obeys Equation (39) with negligible site B magnetisation. In the fast exchange limit $\tau_B << T_{1Br}$, R_r^- in Equation (45) takes the form $R_r^- \cong 1/T_{1Ar} + (p_B/p_A)/T_{1Br} \cong p_A/T_{1Ar} + p_B/T_{1Br}$ of Equation (41).

4.2. Delayed acquisition $s > 0$

4.2.1. Slow exchange limits in the relaxation and acquisition fields B_r and B_a: $1/\tau_{AB} << \min(|\Delta_r|, |\Delta_a|)$

Assume that the slow exchange condition $1/\tau_{AB} << |\Delta_a|$ also holds in the acquisition field B_a though the intrinsic relaxation rates are expected to have values lower than those in the relaxation field $B_r < B_a$ since relaxation rates usually decrease as field increases. For $\Delta_a > 0$, as for the relaxation field B_r, we have $R_a^+ = \alpha_{Aa}$, $R_a^- = \alpha_{Ba}$, $\mu_a^+ \cong 0$, $\mu_a^- \cong \Delta_a\tau_B$, and $D_a = \mu_a^- - \mu_a^+ \cong \Delta_a\tau_B$. Then, dropping all the terms in factors of $1/(|\Delta_r|\tau_B)$ or $1/(|\Delta_a|\tau_B)$, the columns $\tilde{C}^0(s)$, $\tilde{C}^{\pm}(s)$ defined by Equations (23) and (24) reduce to

$$\tilde{C}^0(s) = \begin{pmatrix} \chi_A \\ \chi_B \end{pmatrix} B_a + \begin{pmatrix} e^{-\alpha_{Aa}s}\chi_A \\ e^{-\alpha_{Ba}s}\chi_B \end{pmatrix} (B_r - B_a),$$
$$\tilde{C}^+(s) = m_{Azr}(0) \begin{pmatrix} e^{-\alpha_{Aa}s} \\ 0 \end{pmatrix},$$
$$\tilde{C}^-(s) = m_{Bzr}(0) \begin{pmatrix} 0 \\ e^{-\alpha_{Ba}s} \end{pmatrix}. \quad (48)$$

According to Equation (22), we have

$$M_{Az}(\tau + s) = \chi_A[B_a + e^{-\alpha_{Aa}s}(B_r - B_a)] + m_{Azr}(0)e^{-\alpha_{Aa}s}e^{-\alpha_{Ar}\tau},$$
$$M_{Bz}(\tau + s) = \chi_B[B_a + e^{-\alpha_{Ba}s}(B_r - B_a)] + m_{Bzr}(0)e^{-\alpha_{Ba}s}e^{-\alpha_{Br}\tau}, \quad (49)$$

and the total magnetisation reads

$$M_z(\tau + s) = \chi B_a + (\chi_A e^{-\alpha_{Aa}s} + \chi_B e^{-\alpha_{Ba}s})(B_r - B_a) + m_{Azr}(0)e^{-\alpha_{Aa}s}e^{-\alpha_{Ar}\tau} + m_{Bzr}(0)e^{-\alpha_{Ba}s}e^{-\alpha_{Br}\tau}. \quad (50)$$

4.2.2. Slow exchange limit in the relaxation field B_r and fast exchange limit in the acquisition field B_a: $|\Delta_a| << 1/\tau_{AB} << |\Delta_r|$

This situation may occur since relaxation rates usually decrease as field increases so that $|\Delta_a|$,which is expected to be smaller than $|\Delta_r|$, can become much smaller than $1/\tau_{AB}$. For $\Delta_r > 0$, as in Section 4.1.1, we have $\mu_r^+ \cong 0$, $\mu_r^- \cong \Delta_r\tau_B$ and $D_r = \mu_r^- - \mu_r^+ \cong \Delta_r\tau_B$. As for the fast exchange limit in the relaxation field B_r studied in Section 4.1.2, setting $1/T_{1a} = (1/T_{1Aa} + 1/T_{1Ba})/2$, the effective relaxation rates are $R_a^+ = 1/\tau_A + 1/\tau_B + 1/T_{1a} + (\Delta_a/2)(p_B - p_A)$, $R_a^- \cong p_A/T_{1A} + p_B/T_{1B}$, so that we have $\mu_a^- \cong p_B/p_A$, $\mu_a^+ \cong -1$, $D_a \cong 1/p_A$. Then, neglecting the terms with the factors $1/(|\Delta_r|\tau_B)$, the total magnetisation is given by

$$M_z(\tau + s) = \chi B_a + e^{-R_a^- s}\chi(B_r - B_a) + e^{-R_a^- s}[m_{Azr}(0)e^{-\alpha_{Ar}\tau} + m_{Bzr}(0)e^{-\alpha_{Br}\tau}]. \quad (51)$$

4.2.3. Fast exchange limits in the relaxation and acquisition fields B_r and B_a: $\max(|\Delta_r|, |\Delta_a|) << 1/\tau_{AB}$

Since relaxation rates usually decrease as field increases, it is expected that the condition of fast exchange at field B_r implies the analogous condition $|\Delta_a| = |1/T_{1Aa} - 1/T_{1Ba}| << 1/\tau_{AB}$ of fast exchange at field $B_a > B_r$. As for the fast exchange limit in the relaxation field B_r studied in Section 4.1.2, setting $1/T_{1a} = (1/T_{1Aa} + 1/T_{1Ba})/2$, the effective relaxation rates are $R_a^+ = 1/\tau_A + 1/\tau_B + 1/T_{1a} + (\Delta_a/2)(p_B - p_A)$, $R_a^- \cong p_A/T_{1A} + p_B/T_{1B}$, so that we have $\mu_a^- \cong p_B/p_A$, $\mu_a^+ \cong -1$, $D_a \cong 1/p_A$. The columns $\tilde{C}^0(s)$, $\tilde{C}^{\pm}(s)$ are readily obtained from Equations (23) and (24). Using Equation (22), they yield the site magnetisations

$$M_{Az}(\tau + s) = \chi_A B_a + [(p_B\chi_A - p_A\chi_B)e^{-R_a^+ s} + \chi_A e^{-R_a^- s}](B_r - B_a) + [p_B m_{Azr}(0) - p_A m_{Bzr}(0)]e^{-R_a^+ s}e^{-R_r^+ \tau} + p_A[m_{Azr}(0) + m_{Bzr}(0)]e^{-R_a^- s}e^{-R_r^- \tau},$$
$$M_{Bz}(\tau + s) = \chi_B B_a + [-(p_B\chi_A - p_A\chi_B)e^{-R_a^+ s} + \chi_B e^{-R_a^- s}](B_r - B_a) - [p_B m_{Azr}(0) - p_A m_{Bzr}(0)]e^{-R_a^+ s}e^{-R_r^+ \tau} + p_B[m_{Azr}(0) + m_{Bzr}(0)]e^{-R_a^- s}e^{-R_r^- \tau}, \quad (52)$$

and the total magnetisation

$$M_z(\tau + s) = \chi B_a + \chi e^{-R_a^- s}(B_r - B_a) + [m_{Azr}(0) + m_{Bzr}(0)]e^{-R_a^- s}e^{-R_r^- \tau}. \quad (53)$$

4.2.4. Site of scarce nuclei with high intrinsic relaxation rates in the relaxation and acquisition fields B_r and B_a

Under the same conditions as in Section 4.1.3 and the hypothesis $1/T_{1Aa} << 1/T_{1Ba}$, the site magnetisations

can be approximated as

$$M_{Az}(\tau + s) = \chi_A B_a + e^{-R_a^- s}\chi_A(B_r - B_a) + m_{Azr}(0)e^{-R_a^- s}e^{-R_r^- \tau},$$
$$M_{Bz}(\tau + s) = 0, \quad (54)$$

so that the total magnetisation is

$$M_z(\tau + s) \cong M_{Az}(\tau + s) \cong \chi B_a + e^{-R_a^- s}\chi(B_r - B_a) + m_{zr}(0)e^{-R_a^- s}e^{-R_r^- \tau}. \quad (55)$$

The $M_z(\tau)$ evolution of Equation (55) overlaps time decays obtained in the slow and fast exchange limits. For slow exchange in both fields B_r and B_a, Equation (55) becomes Equation (50) where the site B magnetisation terms in $m_{Bzr}(0)$ and χ_B are neglected. For fast exchange in both fields B_r and B_a, Equation (55) is identical to Equation (53).

As a rule, in the various cases of slow exchange in the fields B_r and/or B_a, when either the intrinsic relaxation rate or the exchange rate is dominant for a given site, note that the α parameter giving the evolution of the site magnetisation is practically equal to the dominant term.

Finally, our formalism using the general evolution operator of the magnetisations of the exchanging sites can be easily applied to any FFC sequence.

5. Relaxometric exploration of systems

Information, that can be deduced from NMR relaxometry, depends on the values of τ_A, τ_B, T_{1Av}, T_{1Bv}. Here, consider typical values of relaxation and residence times in biological systems. The residence time τ_i of an intracellular water molecule is known to vary between 0.01 s for red blood cells to 100 s for xenopus ovocytes [16]. These residence times should be compared with typical intrinsic relaxation times [14]. Whatever the field, the T_1 value is rather long, of the order of 1 s, in the extracellular medium, but can be considerably reduced by inclusion of paramagnetic contrast agents [3–5,11,21]. On the other hand, T_1 drops from 1 s to 30 ms when the field decreases from 0.25 T to 0.2 mT in mouse leg tissues. It should be emphasised that the detailed balance principle implies a decrease of the residence time τ_e of an extracellular water molecule with the volume fraction of the extracellular space, so that τ_e may become an order of magnitude shorter than τ_i. Thus, the values of τ_A, τ_B, T_{1Av}, T_{1Bv} range between a few milliseconds and a few seconds. They can be easily studied with standard NMR spectrometers, the pulse sequences of which make it possible to analyse the evolution of the nuclear magnetisation over times less than 0.1 ms.

The FFC-NMR investigation of dynamical processes of characteristic times between 1 ms and 1 s becomes problematic when the acquisition delay s is not negligible with respect to the values of τ_A, τ_B, T_{1Ar}, T_{1Br}, T_{1Aa}, T_{1Ba}. In practice, this delay incorporates the duration of the field ramp from B_r to B_a and the time required to ensure the B_a stability. It is only of a few milliseconds on a Stelar FFC relaxometer [1], but can reach a few tens of milliseconds on an MRI scanner [2].

The natural time unit τ_u of systems of nuclei undergoing chemical exchange is the shutter time τ_{AB}, or better

$$\tau_u = 2\tau_{AB}, \quad (56)$$

which reduces to the common residence time $\tau_A = \tau_B$ when the sites A and B have equal populations of nuclei. Therefore, the times τ_A, τ_B, T_{1Ar}, T_{1Br}, T_{1Aa}, T_{1Ba} will be expressed in τ_u units hereafter.

It is necessary to sample the total longitudinal magnetisation $M_z(\tau)$ in the relaxation field B_r at both short and long τ values in order to determine R_r^+ and R_r^-, respectively. The application of a 90° pulse to measure $M_z(\tau)$ is only feasible from the moment when the acquisition field B_a is stable, that is at the end of a delay $s > 0$ after the fast jump of the field value B_v from B_r to a value near the acquisition value B_a which is reached by the rapid change of the current through the magnet coil. Then, the observed signal is proportional to $M_z(\tau + s)$ rather than $M_z(\tau)$, where $M_z(\tau + s)$ is given by Equations (25) and (26), which can be used in the general case to derive the lifetimes and intrinsic relaxation rates of the sites at the relaxation field B_r. According to these equations, this derivation is only possible for a short delay s such as $R_a^{\pm}s$ is not significantly larger than unity. Otherwise, the signal vanishes and the relaxation information is lost. In particular, a bi-exponential decrease of the magnetisation can be reduced to an apparent mono-exponential decay if only one of the two factors $w^+(s)$ or $w^-(s)$ keeps a significant value.

Practically, the magnetisation decay with time τ can be fitted either by a single decreasing exponential or by a linear combination of two such exponentials corresponding in principle to the most general case of Equation (25). However, as shown below, the possibility of observing a bi-exponential decay occurs only in special cases because either exchange tends to lead to effective mono-exponential behaviour or the population of one site is largely dominant. A physico-chemical knowledge of the system of exchanging nuclei must be invoked to decide between these two cases. The M_z general expressions of Equations (25), (29), or its limiting expressions of Equations (39), (50), (51) should be used for bi-exponential decay. Simplified mono-exponential expressions, such as

those of Section 4, can be used for mono-exponential relaxation.

Quite generally, bi-exponential relaxation is observable if the ratio w^+/w^- derived from Equation (26) is neither too small nor too large, typically in the range

$$0.1 \leq w^+/w^- \leq 10. \tag{57}$$

Moreover, the effective relaxation rates R_r^+ and R_r^- given by Equation (6) with $v = r$ should differ significantly in order to be distinguishable from experimental data. This is all the more the case with increasing inaccuracy in the measurements and decreasing number of relaxation periods τ. Typically, the ratio $R_r^+/R_r^- \geq 1$ should satisfy the inequality

$$R_r^+/R_r^- \geq 2. \tag{58}$$

Assume that the relaxation field has a fixed value B_r. We will investigate the domain of the parameters τ_A, τ_B, T_{1Ar}, T_{1Br} for which the total magnetisation has a bi-exponential decay. Introduce the population ratio

$$q = \frac{p_B}{p_A} = \frac{\chi_B}{\chi_A} = \frac{\tau_B}{\tau_A}. \tag{59}$$

In what follows, the optimal ideal situation of immediate acquisition $s = 0$ is considered first. The influence of delayed acquisition $s > 0$ is investigated later.

The domain of bi-exponential decay can be characterised by the only three independent dimensionless parameters q, T_{1Ar}/τ_u, T_{1Br}/τ_u forming a three-dimensional space. In this space, the boundary surfaces of the bi-exponential domain, i.e. $w^+/w^- = 0.1$ (grey boundary) and 10 (blue boundary) with $s = 0$, are shown in Figure 2 as a function of the decimal logarithms of the three parameters. The domain is formed by two zones Z_1 and Z_2 between the grey and blue surfaces. More precise information is given in Figure 3 where plane sections of Figure 2 are displayed for different typical fixed q values. Within each of these plane sections, the frontiers of the dotted area are the traces of the above boundary surfaces corresponding to the conditions of Equation (57). Besides, the contours $w^+/w^- = q$ and $1/q$ appear as black and blue curves, respectively. They show that w^+/w^- ranges between q and $1/q$. They should be considered as matching the $\log T_{1Ar}$ and $\log T_{1Br}$ axes when they are parallel and close to these axes. The areas corresponding to the ratio R_r^+/R_r^- in the intervals [1,2], [2,4], [4,12], [12,20], [20, ∞] are coloured in white, green, yellow, orange and red, respectively.

For $q = 1$, the bi-exponential behaviour occurs in two zones symmetric with respect to the principal diagonal with $0.1 \leq w^+/w^- \leq 10$, but not in the fast exchange area and in a narrow band around $T_{1Br} \cong T_{1Ar}$.

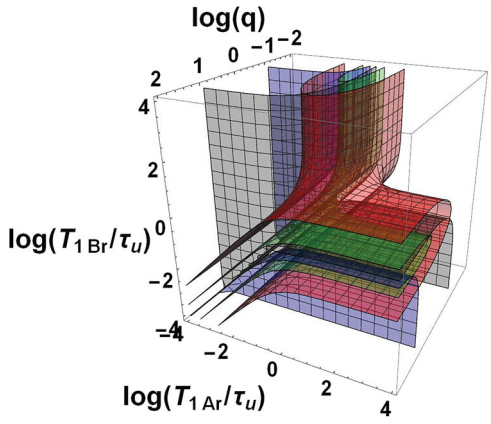

Figure 2. Bi-exponential relaxation domain, $0.1 \leq w^+/w^- \leq 10$, in the space of logarithmic co-ordinates $\log q$ with $q = p_B/p_A$, $\log(T_{1Ar}/\tau_u)$, $\log(T_{1Br}/\tau_u)$ for immediate signal acquisition $s = 0$. This domain is defined by its boundaries $w^+/w^- = 0.1$ (grey contour) and $w^+/w^- = 10$ (blue contour). The surface contours $R_r^+/R_r^- = 3$ (green surface) and $R_r^+/R_r^- = 20$ (red surface) are also displayed (Colour online, B/W in print).

For $q = 0.2$, there are two zones of observable bi-exponential relaxation: a dotted band parallel to the $\log T_{1Ar}$ axis corresponding to $T_{1Br} < T_{1Ar}$ with $0.1 \leq w^+/w^- \leq q = 0.2$ and a dotted band parallel to the $\log T_{1Br}$ axis corresponding to $T_{1Br} > T_{1Ar}$ on the left side of the black curve with $0.1 \leq w^+/w^- \leq 1/q = 5$.

For $q = 5$, the figure is symmetric to the case $q = 0.2$ with respect to the principal diagonal $\log T_{1Ar} = \log T_{1Br}$. The two zones of observable bi-exponential relaxation are a dotted band parallel to the $\log T_{1Ar}$ axis corresponding to $T_{1Br} < T_{1Ar}$ with $0.1 \leq w^+/w^- \leq q = 5$ and a dotted band parallel to the $\log T_{1Br}$ axis corresponding to $T_{1Br} > T_{1Ar}$ below the blue curve with $0.1 \leq w^+/w^- \leq 1/q = 0.2$.

For $q = 0.01$, there is no intersection between the dotted and the coloured zones $R_r^+/R_r^- \geq 2$ indicating the absence of observable bi-exponential relaxation.

For $q = 100$, the figure is symmetric to the case $q = 0.01$ with respect to the principal diagonal $\log T_{1A} = \log T_{1B}$. There is no intersection between the dotted and coloured zones indicating the absence of observable bi-exponential relaxation.

Turn to an instrument with an acquisition delay $s > 0$. For an FFC-MRI scanner with s =20–30 ms, consider residence times τ_A, τ_B of the order of 100–200 ms. Then, a typical acquisition delay is $s/\tau_u = 0.2$. A delay time $s > 0$ leads to an attenuation of the observed signal. Besides this attenuation, the mono or bi-exponential decay of the total magnetisation leads to different qualitative changes. For the cases 4.2.3 and 4.2.4 of mono-exponential decay described by Equations (53) and (55), the attenuation is simply given by the factor $e^{-R_a^- s}$ so that the inequality $R_a^- s \leq 1$ should hold to keep a reasonable signal to

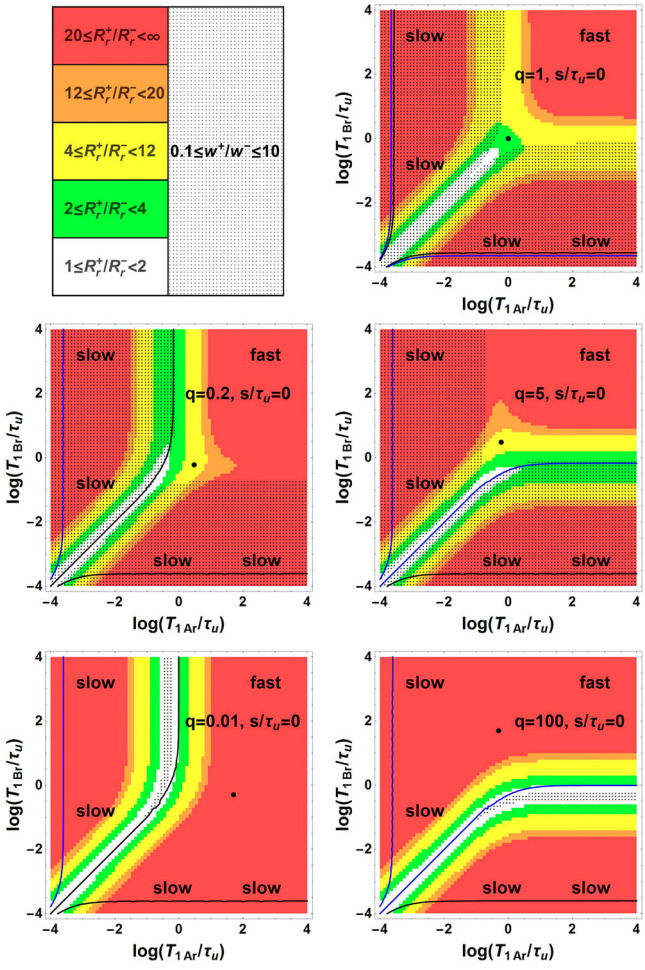

Figure 3. Bi-exponential relaxation areas, $0.1 \leq w^+/w^- \leq 10$, (dotted zones) in the space of logarithmic co-ordinates $\log(T_{1Ar}/\tau_u)$, $\log(T_{1Br}/\tau_u)$ for immediate signal acquisition $s = 0$ and for the values 1, 0.2, 5, 0.01, 100 of the population ratio $q = p_B/p_A = \tau_B/\tau_A$. In the white zone corresponding to $R_r^+/R_r^- < 2$, observation of bi-exponential relaxation is difficult because of the proximity of R_r^+ and R_r^-. Several intervals of the ratio R_r^+/R_r^- (coloured zones) are also displayed. For each q value, the point of co-ordinates $\log(\tau_A/\tau_u)$, $\log(\tau_B/\tau_u)$ is represented by a black circle (Colour online, B/W in print).

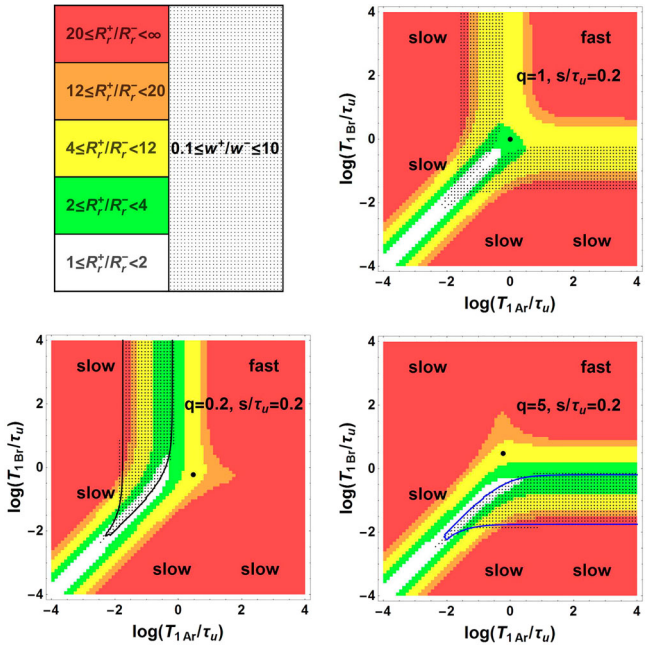

Figure 4. Bi-exponential relaxation areas, $0.1 \leq w^+/w^- \leq 10$, (dotted zones) in the space of logarithmic co-ordinates $\log(T_{1Ar}/\tau_u)$, $\log(T_{1Br}/\tau_u)$ for delayed signal acquisition $s/\tau_u > 0$ and for the values 1, 0.2, 5 of the population ratio $q = p_B/p_A = \tau_B/\tau_A$. The white and coloured areas corresponding to value intervals of R_r^+/R_r^- are defined as in Figure 3. For each q value, the point of co-ordinates $\log(\tau_A/\tau_u)$, $\log(\tau_B/\tau_u)$ is represented by a black circle (Colour online, B/W in print).

noise ratio. The situation is similar for the limiting case 4.2.2 of fast exchange in field B_a and biexponential decay described by Equation (51). By contrast, for the limiting case 4.2.1 of slow exchange in field B_a and bi-exponential decay described by Equation (50), the relative weights of the two exponentials are differently affected. If $R_{1Aa}s > 1$ or $R_{1Ba}s > 1$, the bi-exponential behaviour may reduce to a mono-exponential decay.

The loss of information brought by the delay time $s > 0$ is illustrated in Figure 4 for $q = 1$, 0.2, and 5, where the dotted areas correspond to the condition of bi-exponential decay of Equation (57). Comparing Figure 4(a–c) with the analogous Figure 3(a–c) relative to $s = 0$, the areas corresponding to an observable bi-exponential decay of M_z are considerably reduced. For instance, for $q = 1$, the two symmetric large dotted zones of bi-exponential decay shrink to two symmetrical narrow areas. Moreover, the dotted band parallel to the log T_{1Ar} axis corresponding to $T_{1Br} < T_{1Ar}$ and the dotted band parallel to the log T_{1Br} axis corresponding to $T_{1Br} > T_{1Ar}$ have disappeared for $q = 0.2$ and 5, respectively.

According to extensive previous studies [15], the bi-exponential situation described by the present formalism is likely to occur frequently in biological tissues because the extra- and intra-cellular water molecules have comparable populations. For instance, the extra-cellular/intra-cellular water ratio q is about 1 for blood and brain white matter. In many tissues, it ranges from 0.1 (muscle) to 20 (tumour rim). Moreover, by adding MRI contrast agents at various concentrations into cell suspensions [14,17], the intrinsic relaxation rate of the water protons of the extracellular medium can be significantly increased, making it possible to extract the intrinsic intracellular relaxation rate and the water residence lifetimes in both intra- and extra-cellular compartments by applying the present theory if the acquisition delay is short enough.

The influence of the acquisition delay on the best fit values of residence times and intrinsic relaxation times is

illustrated now by simulating a very-low-field FFC-MRI investigation of a tumour tissue of a mouse leg [14]. Indeed, prototypes of FFC-MRI scanners and FFC-NMR relaxometers operating down to 2 μ T are under development within the framework of the European project IDentIFY. In a tissue, at a given relaxation field B_r, a water molecule basically goes back and forth between the intracellular ($A = in$) space with intrinsic longitudinal time $T_{1in,r}$ during a residence time τ_{in} and the extracellular ($B = ex$) space with intrinsic longitudinal time $T_{1ex,r}$ during a residence time τ_{ex}. The population fractions are assumed to be $p_{ex} = 0.2$ and $p_{in} = 0.8$ since p_{ex}, denoted as V_{ex} in Ref. [14], ranges between 0.14 and 0.30. Since the intracellular lifetime τ_{in} ranges between 0.48 and 1.44 s, we assume $\tau_{in} = 800$ ms and $\tau_{ex} = (p_{ex}/p_{in})\tau_{in} = 200$ ms. Below 0.2 mT, according to Figure 4 of Ref. [14] and to Fig. S2 of the related Supporting Information, $T_{1in,r}$ and $T_{1ex,r}$ are expected to be of the order of a few tens and a few hundreds of ms, respectively. For simulation purpose, at $B_r = 10\ \mu$ T, we take extrapolated values $T_{1in,r} = 20$ ms and $T_{1ex,r} = 400$ ms. The initial proton magnetisation is assumed to have the equilibrium value in the polarisation field $B_p = 100$ mT. The acquisition field is $B_a = 60$ mT, in which the estimates of the intrinsic relaxation times are $T_{1in,a} = 150$ ms and $T_{1ex,a} = 2000$ ms. Finally, the acquisition delay has a typical value $s = 20$ ms as in an MRI scanner built by Lurie *et al.* [2,7–9]. Thus, s is not negligible with respect to both $T_{1in,a}$ and τ_{ex}.

Applying the PP sequence of Figure 1, the evolution of the total magnetisation M_z of the water protons is simulated for the above input parameter values according to Equation (25) which accounts for the acquisition delay. The simulated magnetisation values shown by dots in Figure 5 were obtained for 24 exponentially spaced values of the evolution period τ, ranging between 2 and 700 ms. As in a real experiment, each M_z value is affected by a random error assumed to be here of $\pm 1\%$. Then, the best fit independent parameters p_{ex}^{fit}, τ_{ex}^{fit}, $T_{1in,r}^{fit}$, $T_{1ex,r}^{fit}$ entering the magnetisation $M_z(\tau + s)$ in Equation (25) are expected to deviate from the 'true' input values $p_{ex} = 0.2$, $\tau_{ex} = 200$ ms, $T_{1in,r} = 20$ ms, $T_{1ex,r} = 400$ ms. Even for the present small simulated 'experimental' uncertainties and despite the excellent agreement between the continuous fitted function $M_z(\tau + s)$ and the simulated data shown in Figure 5, several best-fit parameters $p_{ex}^{fit} = 0.235$, $\tau_{ex}^{fit} \to \infty$, $T_{1in,r}^{fit} = 19.8$ ms, $T_{1ex,r}^{fit} = 146$ ms are significantly different from the input values. In particular, the best-fit residence times have very large values so that there is practically no water exchange. Now, following Ruggiero *et al.* [14], assume that the extracellular medium is similar to Matrigel and has the known value $T_{1ex,r}^{fit} = 400$ ms obtained in Matrigel from independent FFC-NMR measurements. Under these conditions, we obtain $p_{ex}^{fit} = 0.195 \pm 0.01$, $\tau_{ex}^{fit} = 209 \pm 18$ ms, $T_{1in,r}^{fit} = 20.3 \pm 0.4$ ms in very good agreement with the input values and still an excellent agreement between the continuous fitted function $M_z(\tau + s)$ and the simulated data as shown in Figure 5. Note that the simulated data cannot be reproduced by the mono-exponential fit represented by the dashed curve in Figure 5.

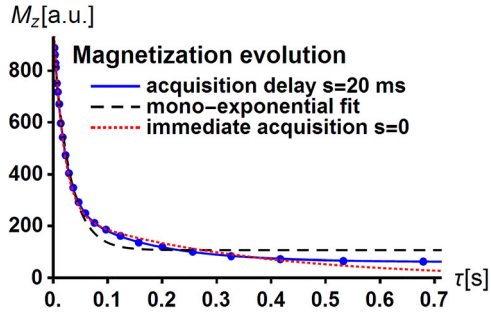

Figure 5. Typical bi-exponential time decay of the water proton magnetisation of a tumour tissue of a mouse leg at body temperature in the relaxation field $B_r = 10\ \mu$ T of an FFC-MRI scanner. Water molecule basically goes back and forth between the intracellular space and the extracellular space. The discrete dots are the simulated data corresponding to $M_z(\tau + s)$ in Equation (25) with realistic exchange and relaxation input parameters (see text) for an acquisition delay $s = 20$ ms with random magnetisation errors of $\pm 1\%$. The superimposed continuous curves are the excellent fits of $M_z(\tau + s)$ to the previous simulated data (see text). The dashed curve is the unsuccessful mono-exponential relaxation function fitted to the simulated data. The dotted curve is the poor fit of $M_z(\tau)$ ($s = 0$) in Equation (29) to the simulated data.

Turn to the influence of the acquisition delay on the best-fit parameters. Here, the simulated data are still those which were previously obtained by using the magnetisation $M_z(\tau + s)$ of Equation (25) with acquisition delay $s = 20$ ms, but the fitted function is the magnetisation $M_z(\tau)$ of Equation (29) with immediate acquisition $s = 0$. Setting $T_{1ex,r}^{fit} = 400$ ms, the best-fit parameters $p_{ex}^{fit} = 0.242$, $\tau_{ex}^{fit} = 1650$ ms, $T_{1in,r}^{fit} = 19$ ms are in strong disagreement with the input values and lead to a fitted function $M_z(\tau)$, represented in Figure 5 by a dotted curve which also strongly departs from the simulated data. For $s = 0$, even if the amplitude of $M_z(\tau)$ is considered as an additional adjustable parameter through an additive term c_0, the fit agreement is not improved. This simple example shows that the influence of the acquisition delay on the best-fit parameters of the magnetisation expressions should be carefully examined in systems with bi-exponential decay as soon as it somewhat affects the observed magnetisation.

Finally, recent theoretical developments in the analysis of multi-exponential relaxation data [22] should facilitate the precise determination of the physico-chemical parameters involved in systems of nuclear spins undergoing chemical exchange.

6. Conclusion

We have presented a general formalism for describing the evolution of the magnetisations of populations of nuclei exchanging between two sites after an FFC sequence. In the case of the PP sequence, we have derived general expressions of the magnetisation decay and provided simple formulas in the slow and fast exchange limits, and in the case of a site of scarce nuclei with high intrinsic relaxation rate. We have shown that a bi-exponential decay is only observable if both site populations are comparable and if the exchange rates are slower than or comparable to the absolute difference of intrinsic relaxation rates. We have given analytic expressions of the loss of information due to the finite acquisition delay. We have shown that the acquisition delay can strongly affect the fitted values of the populations, residence times, and intrinsic relaxation times of the sites in the case of bi-exponential relaxation.

Disclosure statement

No potential conflict of interest was reported by the authors.

Funding

This work was supported by the European Union Horizon 2020 research and innovation programme under grant agreement no. 668119 (project 'IDentIFY'), and was performed under the auspices of the COST Action AC15209, EURELAX.

References

[1] G. Ferrante and S. Sykora, Adv. Inorg. Chem. **507**, 405 (2005).
[2] D.J. Lurie, S. Aime, S. Baroni, N.A. Booth, L.M. Broche, C.-H. Choi, G.R. Davies, S. Ismail, D.Ó. Hógáin and K.J. Pine, C. R. Phys. **11**, 136 (2010).
[3] L. Banci, I. Bertini and C. Luchinat, Nuclear and Electron Relaxation: The Magnetic Nucleus-Unpaired Electron Coupling in Solution (VCH, Weinheim, 1991).
[4] I. Bertini, C. Luchinat and G. Parigi, Solution NMR of Paramagnetic Molecules (Elsevier, Amsterdam, 2001).
[5] C.S. Bonnet, P.H. Fries, S. Crouzy and P. Delangle, J. Phys. Chem. B **114**, 8770 (2010).
[6] A.L. Rollet, S. Neveu, P. Porion, V. Dupuis, N. Cherrak and P. Levitz, Phys. Chem. Chem. Phys. **18**, 32981 (2016).
[7] D. Kruk, M. Wojciechowski, Y.L. Verma, S.K. Chaurasia and R.K. Singh, Phys. Chem. Chem. Phys. **19**, 32605 (2017).
[8] K. Venu, V.P. Denisov and B. Halle, J. Am. Chem. Soc. **119**, 3122 (1997).
[9] E. Persson and B. Halle, Proc. Natl. Acad. Sci. **105**, 6266 (2008).
[10] E. Ravera, G. Parigi, A. Mainz, T.L. Religa, B. Reif and C. Luchinat, J. Phys. Chem. B **117**, 3548 (2013).
[11] D.Ó. Hógáin, G.R. Davies, S. Baroni, S. Aime and D.J. Lurie, Phys. Med. Biol. **56**, 105 (2011).
[12] L.M. Broche, S.R. Ismail, N.A. Booth and D.J. Lurie, Magn. Reson. Med. **67**, 1453 (2012).
[13] L.M. Broche, G.P. Ashcroft and D.J. Lurie, Magn. Reson. Med. **68**, 358 (2012).
[14] M.R. Ruggiero, S. Baroni, S. Pezzana, G. Ferrante, S. Geninatti Crich and S. Aime, Angew. Chem. Int. Ed. **57**, 7468 (2018).
[15] C.S. Landis, X. Li, F.W. Telang, P.E. Molina, I. Palyka, G. Vetek and C.S. Springer, Jr., Magn. Reson. Med. **42**, 467 (1999).
[16] C.S. Springer, Jr., X. Li, L.A. Tudorica, K.Y. Oh, N. Roy, S.Y-C. Chui, A.M. Naik, M.L. Holtorf, A. Afzal, W.D. Rooney and W. Huang, NMR Biomed. **27**, 760 (2014).
[17] E. Gianolio, G. Ferrauto, E. Di Gregorio and S. Aime, Biochim. Biophys. Acta **1858**, 627 (2016).
[18] G.J. Béné, Helv. Phys. Acta **61**, 572 (1988).
[19] H.M. McConnell, J. Chem. Phys. **28**, 430 (1958).
[20] A.C. McLaughlin and J.S. Leigh, Jr., J. Magn. Reson. **9**, 296 (1973).
[21] J. Kowalewski and L. Mäler, Nuclear Spin Relaxation in Liquids: Theory, Experiments, and Applications (Taylor & Francis, New York, 2006).
[22] O.V. Petrov and S. Stapf, J. Magn. Reson. **279**, 29 (2017).